Clays and Clay Minerals, Vol. 45, No. 3, 418–427, 1997.

QUANTITATIVE PHASE ANALYSIS OF BIDI-KOUM BAUXITES (GUINEA)

FRANK FERET,[1] MONIQUE AUTHIER-MARTIN[1] AND ISTVÁN SAJÓ[2]

[1] Alcan International Ltd, Arvida Research and Development Centre, Jonquière, Québec, Canada G7S 4K8

[2] Bay Zoltan Institute for Materials Science and Engineering, H-1116 Budapest, Fehervati ut 130, Hungary

Abstract—Fifty-two Bidi-Koum bauxites from Guinea, Africa, of diversified chemical composition were characterized for their mineral composition. First, 14 element oxide concentrations were determined by X-ray fluorescence (XRF) using a fusion sample preparation technique. Loss of Mass (LOM) and organic carbon (OC) concentrations were also determined. The initial X-ray diffraction (XRD) phase quantification was carried out employing XDB software. This software allows for full interpretation of a sample diffractogram and helps generate initial concentrations of identified minerals based on a standardless approach. In the stage that followed, the mass balance procedure on the XDB software helped refine the final phase composition. Then, gibbsitic Al_2O_3 concentrations obtained by wet chemistry for all samples and kaolinitic SiO_2 concentrations obtained for selected samples were compared with the concentrations obtained using the XDB software. Phases that were quantified are: gibbsite, boehmite, kaolinite, wavellite, goethite, hematite, quartz, anatase, rutile and illite. Phase concentrations were obtained for illite from K_2O and for wavellite from P_2O_5 concentrations. The alumina substitution in the goethite lattice was also estimated.

Key Words—Bauxite, Boehmite, Gibbsite, Goethite, Hematite, Quantitative Phase Analysis, Wet Chemistry, X-ray Diffraction, X-ray Fluorescence.

INTRODUCTION

An accurate estimate of bauxite exploration and supply is important for the efficient operation of a mine and a Bayer plant. Traditional methods used to determine bauxite phase composition are based on wet chemistry. Compared with wet chemistry, XRD offers speed and a much lower cost of analysis, but is less accurate. A typical XRD analysis (Black 1953; Andrews and Crisp 1980; Bárdossy et al. 1980; Strahl 1982; Bredell 1983; Montgomery and deFoggi 1983; Schorin and Carias 1987; Boski and Herbillon 1988) is based on a calibration established using a series of calibration standards closely matching mineralogy of the unknowns. The typical methods are matrix-specific, so that developed equations may not apply to other bauxite deposits. Moreover, they are limited to the concentration ranges of variables for which the calibration coefficients were calculated. The minerals that are the most critical to this analysis, such as gibbsite, goethite or kaolinite, show wide variations in XRD response due to natural diversification in crystallinity, poor crystallinity and preferred orientation. Phase quantification methods involving regression (Feret and Giasson 1991) may successfully be used in bauxite exploration, but they too are deposit-specific.

Over the last few years, 2 distinct approaches that do not depend on any calibration standards have emerged in modern XRD quantitative phase analysis. One approach is based on the Rietveld least-square refinements and is already represented by a number of commercial programs (Taylor 1991; Hill 1992; Young 1993). Unfortunately, the Rietveld approach is hampered mostly by the amorphous phases, solid solutions and gibbsite preferred-orientation effect. For this study, the XDB software (Solymár et al. 1991; Sajó 1994) was employed. It uses chemical information available on the sample [XRF or inductively coupled plasma (ICP), wet chemistry as well as LOM data] in addition to the XRD pattern. The XRD intensities and experimental constants that characterize absorption of an individual mineral help obtain initial phase composition. In the final analysis, some significant concentration refinements are accomplished using a mass balance approach. In the mass balance, the chemical composition of the identified mineralogical components is compared with known LOM and elemental concentrations. A model of the sample XRD pattern can also be produced by compiling data from each of the identified minerals.

The objective of this work was to determine the phase composition of representative Bidi-Koum bauxites (Guinea, Africa) and advance understanding of their mineralogy. Another objective was to compare selected concentrations obtained by wet chemistry and estimated by the XDB software.

METHODS AND RESULTS

Determinations by XRF, Wet Chemistry and XRD

Fifty-two Bidi-Koum samples from the Boké region were used in the study. All samples were 1st analyzed for elemental composition in Alcan's Research and Development Centre (ARDC), as well as in the Centre de Recherche Minérales (CRM) in Quebec. In both labo-

Copyright © 1997, The Clay Minerals Society

https://doi.org/10.1346/CCMN.1997.0450311 Published online by Cambridge University Press

Table 1. Major oxide concentrations (%).

Sample	Al_2O_3	SiO_2	Fe_2O_3	TiO_2	P_2O_5	K_2O	H_2O	Sum
BDK 1	50.2	0.84	19.9	2.66	0.17	0.02	25.3	99.0
BDK 2	49.0	0.84	20.7	2.7	0.15	0.02	25.7	99.1
BDK 3	53.0	0.8	15.4	2.85	0.13	0.02	26.7	99.0
BDK 4	44.1	1.34	27.3	2.54	0.18	0.03	23.8	99.2
BDK 5	57.5	0.73	8.7	3.37	0.08	0.01	29.1	99.5
BDK 6	56.3	0.55	10.0	2.88	0.095	0.01	29.4	99.3
BDK 7	53.5	1.21	13.5	2.38	0.08	0.02	28.8	99.5
BDK 8	55.7	1.49	10.2	2.69	0.1	0.02	29.0	99.2
BDK 9	59.4	1.01	4.9	2.98	0.09	0.01	31.0	99.3
BDK 10	51.4	1.43	16.9	2.42	0.165	0.02	26.8	99.2
BDK 11	43.3	1.02	28.3	2.17	0.32	0.01	24.3	99.4
BDK 12	44.6	1.16	24.7	4.1	0.18	0.01	24.2	99.0
BDK 13	49.3	0.62	17.2	4.9	0.13	0.01	26.9	99.1
BDK 14	46.8	1.14	21.5	4.3	0.18	0.01	25.1	99.0
BDK 15	56.6	0.58	7.3	4.26	0.09	0.01	30.4	99.2
BDK 16	58.4	0.49	5.3	4.25	0.04	0.01	30.9	99.3
BDK 17	60.2	0.56	3.1	3.65	0.035	0.01	31.7	99.3
BDK 18	54.2	0.48	11.0	4.1	0.165	0.01	29.2	99.2
BDK 19	53.8	0.48	12.5	3.8	0.195	0.01	28.2	99.0
BDK 20	56.7	0.43	6.4	5.96	0.09	0.01	29.5	99.0
BDK 21	56.9	0.36	7.0	4.48	0.09	0.01	30.4	99.2
BDK 22	57.1	0.43	7.8	3.21	0.07	0.01	30.7	99.3
BDK 23	59.3	0.51	5.1	2.84	0.04	0.02	31.6	99.4
BDK 24	57.3	0.41	8.1	2.84	0.045	0.01	30.7	99.3
BDK 25	52.8	1.33	13.7	3.04	0.1	0.02	28.1	99.2
BDK 26	53.2	1.19	12.9	2.94	0.11	0.02	28.8	99.2
BDK 27	50.1	1.17	16.8	3.7	0.115	0.02	27.2	99.1
BDK 28	58.9	1.1	6.4	3.5	0.07	0.005	29.6	99.5
BDK 29	53.8	0.85	11.0	5.04	0.115	0.005	28.4	99.2
BDK 30	61.3	0.36	3.0	4.55	0.055	0.005	30.1	99.3
BDK 31	58.5	0.69	4.6	5.69	0.06	0.005	29.9	99.4
BDK 32	52.6	2.22	13.1	3.28	0.15	0.01	27.8	99.1
BDK 33	33.7	6.89	37.7	2.04	0.145	0.13	18.6	99.1
BDK 39	31.8	2.33	44.1	1.56	0.3	0.03	19.2	99.3
BDK 41	40.5	2.89	32.3	1.87	0.31	0.03	21.5	99.4
BDK 42	41.2	5.11	28.7	1.58	0.55	0.06	22.4	99.6
BDK 43	43.3	2.83	27.2	2.37	0.94	0.02	22.6	99.2
BDK 44	46.4	0.66	24.7	2.51	0.21	0.005	25.0	99.4
BDK 45	52.1	0.55	15.0	3.92	0.14	0.005	27.6	99.3
BDK 46	54.1	0.76	12.1	3.59	0.13	0.01	28.5	99.1
BDK 47	56.1	0.73	8.3	4.63	0.12	0.005	29.5	99.3
BDK 48	58.1	0.65	6.1	3.89	0.11	0.005	30.4	99.2
BDK 49	59.2	0.34	2.4	6.6	0.06	0.005	30.7	99.3
BDK 50	59.6	1.06	4.1	4.18	0.08	0.005	30.5	99.5
BDK 51	62.8	0.4	5.9	3.42	0.11	0.005	26.7	99.3
BDK 52	58.5	0.94	5.1	3.48	0.11	0.005	30.3	98.4
BDK 34	12.9	23.00	51.7	0.68	0.18	1.22	9.8	99.4
BDK 35	11.7	30.50	46.0	0.63	0.17	1.36	9.0	99.3
BDK 36	15.9	12.40	56.3	0.91	0.34	0.88	12.7	99.4
BDK 37	25.7	40.50	19.6	1.3	0.2	2.45	8.8	98.5
BDK 38	28.3	54.10	4.4	1.62	0.1	3.22	7.8	99.5
BDK 40	35.0	43.7	5.2	1.71	0.08	3.48	10.1	99.3

ratories, XRF and the fusion sample preparation technique (Feret 1993) were used. The major oxide concentrations and H_2O are given in Table 1. The %LOM values were determined by sample calcination at 1000 °C. The H_2O concentrations listed in Table 1 were obtained by subtracting OC from the LOM values. The OC contributions varied from 0.04 to 0.20%. All other element oxides usually analyzed in bauxites such as MgO, CaO, MnO, ZnO, ZrO_2, Cr_2O_3, V_2O_5 and Na_2O were present at low concentration. The last column in Table 1 shows that the sum of 6 major bauxite constituents considered in this work and H_2O, averages 99.4%. This also confirms that the sum of the remaining secondary constituents is low and varies slightly.

Initial XRD phase quantification employed XDB software and used only sample diffractograms, LOM

https://doi.org/10.1346/CCMN.1997.0450311 Published online by Cambridge University Press

Table 2. Bidi-Koum phase composition (%).

Sample	Gibb	Boeh	Kaol	Wave	Goet	Hema	Quar	TiO_2	Illi	Sum
BDK 1	63.5	7.5	1.5	0.49	17.1	6.1	0.06	2.66	0.21	99.1
BDK 2	65.0	4.6	1.5	0.44	20.4	4.4	0.07	2.70	0.21	99.2
BDK 3	68.9	7.0	1.5	0.38	14.0	4.2	0.03	2.85	0.21	99.0
BDK 4	56.7	5.3	2.5	0.52	26.4	5.0	0.04	2.54	0.32	99.3
BDK 5	78.8	5.9	1.3	0.23	6.8	3.0	0.10	3.37	0.11	99.6
BDK 6	81.2	2.6	0.9	0.28	6.7	4.7	0.08	2.88	0.11	99.3
BDK 7	78.1	0.4	2.3	0.23	11.9	4.0	0.07	2.38	0.21	99.5
BDK 8	78.8	3.0	2.9	0.29	7.3	4.1	0.05	2.69	0.21	99.3
BDK 9	86.5	1.8	1.8	0.26	4.3	1.5	0.13	2.98	0.11	99.4
BDK 10	68.4	4.6	2.7	0.48	18.1	2.3	0.10	2.42	0.21	99.3
BDK 11	61.7	1.0	1.5	0.93	21.6	10.2	0.29	2.17	0.11	99.4
BDK 12	61.5	1.9	2.0	0.52	20.7	8.1	0.20	4.10	0.11	99.0
BDK 13	71.1	0.8	0.9	0.38	18.1	2.7	0.15	4.90	0.11	99.1
BDK 14	64.4	2.4	2.1	0.52	18.9	6.3	0.14	4.30	0.11	99.1
BDK 15	84.9	0.1	0.9	0.26	6.6	2.0	0.10	4.26	0.11	99.2
BDK 16	87.7	0.5	0.9	0.12	2.4	3.4	0.03	4.25	0.11	99.4
BDK 17	90.1	0.7	1.0	0.10	2.6	1.0	0.05	3.65	0.11	99.3
BDK 18	78.9	0.6	0.9	0.48	13.3	0.8	0.01	4.10	0.11	99.1
BDK 19	75.0	3.0	0.8	0.57	14.4	1.4	0.08	3.80	0.11	99.1
BDK 20	81.8	2.7	0.6	0.26	6.4	1.4	0.10	5.96	0.11	99.3
BDK 21	84.4	1.2	0.5	0.26	7.6	0.7	0.06	4.48	0.11	99.3
BDK 22	85.1	0.4	0.7	0.20	8.7	0.8	0.05	3.21	0.11	99.3
BDK 23	88.4	0.7	0.9	0.09	6.2	0.1	0.01	2.84	0.21	99.4
BDK 24	84.6	1.0	0.6	0.13	9.5	0.5	0.06	2.84	0.11	99.3
BDK 25	74.4	2.1	2.5	0.29	15.1	1.6	0.09	3.04	0.21	99.2
BDK 26	78.0	0.2	2.2	0.32	12.9	2.5	0.10	2.94	0.21	99.3
BDK 27	70.2	1.8	1.7	0.33	20.8	0.1	0.29	3.70	0.21	99.1
BDK 28	79.2	6.6	1.9	0.20	7.6	0.4	0.20	3.50	0.05	99.6
BDK 29	75.7	1.8	1.5	0.32	14.2	0.4	0.13	5.04	0.05	99.1
BDK 30	81.8	8.6	0.5	0.16	2.9	0.7	0.09	4.55	0.05	99.3
BDK 31	81.9	4.0	1.1	0.17	6.1	0.3	0.13	5.69	0.05	99.3
BDK 32	73.0	3.0	3.9	0.44	13.6	1.6	0.35	3.28	0.11	99.2
BDK 33	42.0	0.8	11.9	0.42	19.0	20.8	0.70	2.02	1.40	99.0
BDK 39	41.4	1.8	4.3	0.87	36.1	12.9	0.19	1.56	0.32	99.4
BDK 41	56.0	1.6	5.1	0.90	8.1	25.3	0.40	1.87	0.32	99.5
BDK 42	53.7	1.5	9.0	1.60	17.1	13.9	0.63	1.58	0.63	99.5
BDK 43	52.5	5.8	5.2	2.73	18.8	11.3	0.31	2.37	0.21	99.1
BDK 44	62.8	3.2	1.2	0.61	22.3	6.7	0.08	2.51	0.05	99.4
BDK 45	74.3	2.4	1.0	0.41	11.0	6.1	0.06	3.92	0.05	99.2
BDK 46	76.5	3.1	1.2	0.38	11.4	2.8	0.15	3.59	0.11	99.2
BDK 47	81.3	2.2	1.3	0.35	6.1	3.4	0.13	4.63	0.05	99.4
BDK 48	84.9	2.0	1.0	0.32	3.6	3.4	0.14	3.89	0.05	99.2
BDK 49	86.8	2.3	0.6	0.17	1.5	1.2	0.06	6.60	0.05	99.2
BDK 50	85.1	3.5	1.9	0.23	1.4	2.9	0.18	4.18	0.05	99.4
BDK 51	63.9	22.7	0.7	0.32	7.5	0.7	0.05	3.42	0.05	99.2
BDK 52	83.4	2.8	1.4	0.32	6.5	0.3	0.27	3.48	0.05	98.5
BDK 34	2.5	0.0	14.9	0.52	56.7	1.0	10.22	0.68	12.9	99.4
BDK 35	5.1	0.0	6.8	0.49	50.7	0.5	20.83	0.63	14.4	99.3
BDK 36	11.4	0.0	11.5	0.99	61.2	1.3	2.84	0.91	9.3	99.4
BDK 37	0.3	0.0	34.6	0.58	17.8	5.3	12.67	1.30	25.9	98.4
BDK 38	0.0	1.5	33.7	0.29	4.1	1.2	23.01	1.62	34.0	99.4
BDK 40	0.2	1.0	52.4	0.23	1.5	3.9	2.66	1.71	36.7	99.3

and most elemental concentrations. The chemically determined phase concentrations [g.Al_2O_3 (gibbsitic alumina), b.Al_2O_3 (boehmitic alumina) and k.SiO_2 (kaolinitic silica)] were then obtained from 2 independent analysts for most samples. For samples for which the wet chemical data on k.SiO_2 and b.Al_2O_3 were not available, the initial XRD phase composition was refined in ARDC using the g.Al_2O_3 determined by wet chemistry and the XDB software. The illite and wavellite concentrations were calculated based on the K_2O (illite) and P_2O_5 (wavellite) concentrations known from XRF analysis. The phase composition of Bidi-Koum bauxites considered in the study is listed in Table 2. The sum of anatase and rutile is reported as TiO_2 in Table 2. Samples BDK 34–38 and BDK 40 listed in the end of Table

https://doi.org/10.1346/CCMN.1997.0450311 Published online by Cambridge University Press

Table 3. Summary of determinations for phase composition.

Determination	Method used	Samples analyzed	Additional determinations with *XDB* software
g.Al_2O_3	Wet chemistry	1–52	34–38, 40
b.Al_2O_3	Wet chemistry	34–52	1–52
k.SiO_2	Wet chemistry	1–33	34–52
Quartz	XRD	—	1–52
Illite	XRF (K)	1–52	34–43
Hematite	XRD†	1–33	1–52
Goethite	XRD	—	1–52
Anatase	XRD	—	1–52
Rutile	XRD	—	1–52
Wavellite	XRF (P)	1–52	—

† XRD calibration was accomplished by a standard addition method.

2 are clearly non-bauxitic but provide valuable information on secondary phases. A summary of all determinations for phase composition is given in Table 3.

Determination of Illite

The secondary elements are important in the phase quantification of Bidi-Koum bauxites and cannot be ignored. For example, in several samples low in Al_2O_3, a relatively high content of K_2O was obtained. Potassium was matched with illite clearly identified in the diffractograms. Figure 1 shows a diffractogram of a non-bauxitic sample (BDK 40) with kaolinite and illite as the major phases. The illite ($(K,H_3O)Al_2Si_3AlO_{10}(OH)_2$) content was calculated using the formula:

$$\% \text{ Illite} = 10.56\ K_2O\ (\%) \quad [1]$$

In all bauxitic samples the typical K_2O content was 0.01%.

Quantification of Wavellite

Another interesting secondary element is phosphorus. The P_2O_5 content determined by XRF ranges from 0.04 to 0.94% (BDK 34), but is mostly at the 0.15% level. Phosphorus in bauxite samples is usually associated with a calcium aluminum phosphate phase called "crandallite" or "pseudo-wavellite". However, a very low CaO content (0.02% and less) in all except 1 sample practically precludes crandallite from occurring. No phosphate-bearing mineral could have been identified on the diffractograms due to low content. Therefore, it was assumed that, in bauxites from the Bidi-Koum region, phosphorus is present as wavellite, $(Al_2O_3)_3{\cdot}(P_2O_5)_2{\cdot}13H_2O$, a hydrated aluminum phosphate readily decomposed under low-temperature digestion conditions. Table 2 gives the calculated values of wavellite based on % P_2O_5. The concentrations were calculated using the stoichiometric relationship:

$$\% \text{ Wavellite} = 2.903\ P_2O_5\ (\%) \quad [2]$$

In a few samples low in Al_2O_3, the P_2O_5 content was relatively high, resulting in important w.Al_2O_3 contributions in the alumina balance and w.H_2O contribu-

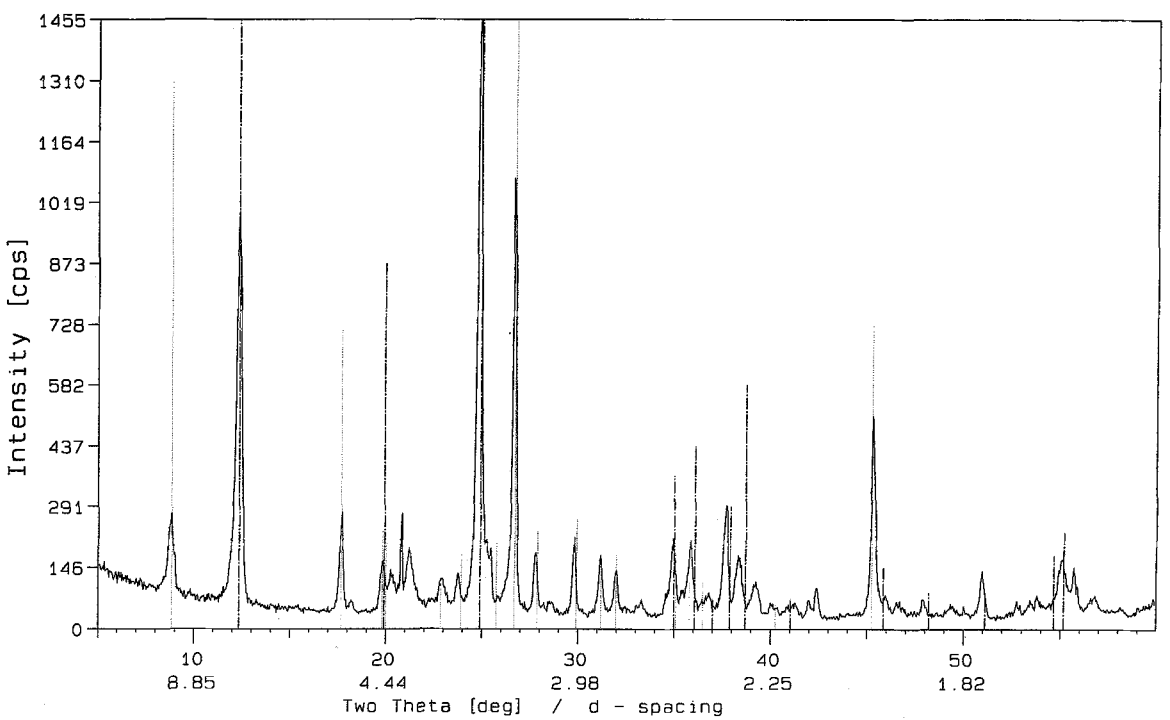


Figure 1. Diffractogram of a non-bauxitic sample (BDK 40) showing kaolinite and illite.

https://doi.org/10.1346/CCMN.1997.0450311 Published online by Cambridge University Press

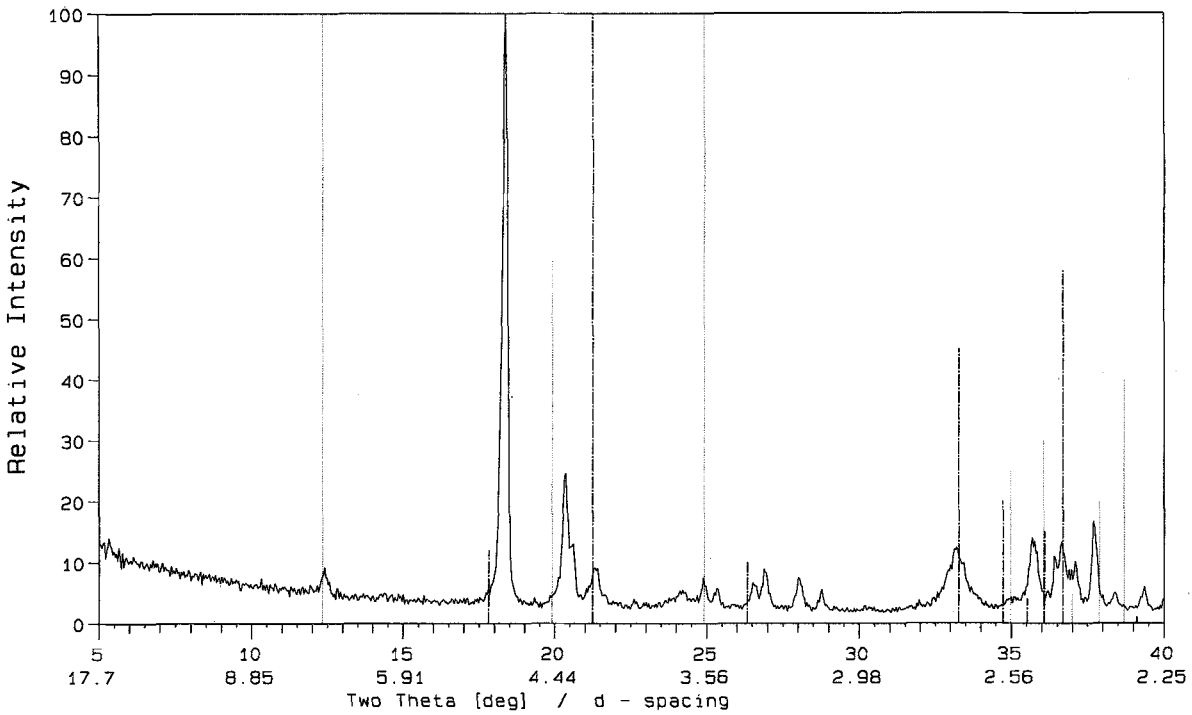


Figure 2. Diffractogram of BDK 42 showing weak peaks of kaolinite (9.0%) and goethite (17.1%).

tions in the water balance. The highest wavellite content of 2.73% was obtained for sample BDK 43, based on P_2O_5 = 0.94%. It has to be realized that wavellite is just a hypothetical compound, not confirmed on diffractograms. It was used in order to complete the mass balance calculations. Most likely, phosphorus may be adsorbed as a binuclear bridging surface complex on contiguous hydroxyls of the goethite crystal faces by forming bonds to the surface oxide ions.

Determination of Kaolinite

The k.SiO_2 was determined in a standard low-temperature caustic digestion in a Parr bomb. Kaolinitic silica is the amount of silica reacting with the liquor and passing 1st into the solution and then precipitating as an acid soluble alumino-silicate, Bayer sodalite. As far as is known, it is mainly the kaolinite-type minerals that will dissolve under the digestion conditions. Quartz will not dissolve, unless exceptionally finely divided or poorly crystallized. Therefore, it was assumed that any silica not dissolving under these conditions represents quartz, plus other rarely detected by XRD clay-type silicates, such as albite ($NaAlSi_3O_8$), anorthite ($CaAl_2Si_2O_8$), orthoclase ($KAlSi_3O_8$), sanidine $(Na,K)AlSi_3O_8$ or zircon ($ZrSiO_4$). The amount of these silicates is insignificant, given the low content of the secondary elements in the analyzed samples. For a number of samples for which the k.SiO_2 determined by wet chemistry was below 1.5%, the XRD analysis did not show the kaolinite peak at all. No other corresponding mineral was identified. This means that in these samples kaolinite is likely amorphous. Moreover, the size of the strongest quartz peak at 3.34 Å could not justify all the SiO_2 found in these samples by XRF. Figure 2 shows a diffractogram of BDK 42 highlighting peaks of kaolinite and goethite. Both peaks are relatively weak despite significant concentration of the respective phases: kaolinite (9.0%) and goethite (17.0%). The k.SiO_2 concentrations for samples BDK 34–52 were obtained in composition simulations with the XDB software using the g.Al_2O_3 concentrations determined by wet chemistry.

Determination of Gibbsite

The g.Al_2O_3 is determined during the low-temperature digestion (~150 °C) with caustic. It is believed that a large part of any phosphates present dissolves along with gibbsite in the digestion process. In order to be able to compare g.Al_2O_3 obtained with different methods (including XRD), it was assumed that:

$$\%\ \text{g.Al}_2\text{O}_3\ (\sim 150\ ^\circ\text{C}) = \text{g.Al}_2\text{O}_3 + \text{w.Al}_2\text{O}_3 \quad [3]$$

where w.Al_2O_3 = alumina in wavellite. The wet chemical concentrations of gibbsite (recalculated from g.Al_2O_3) are compared with the XDB data in Figure 3. The standard deviation for this correlation is 0.99%.

https://doi.org/10.1346/CCMN.1997.0450311 Published online by Cambridge University Press

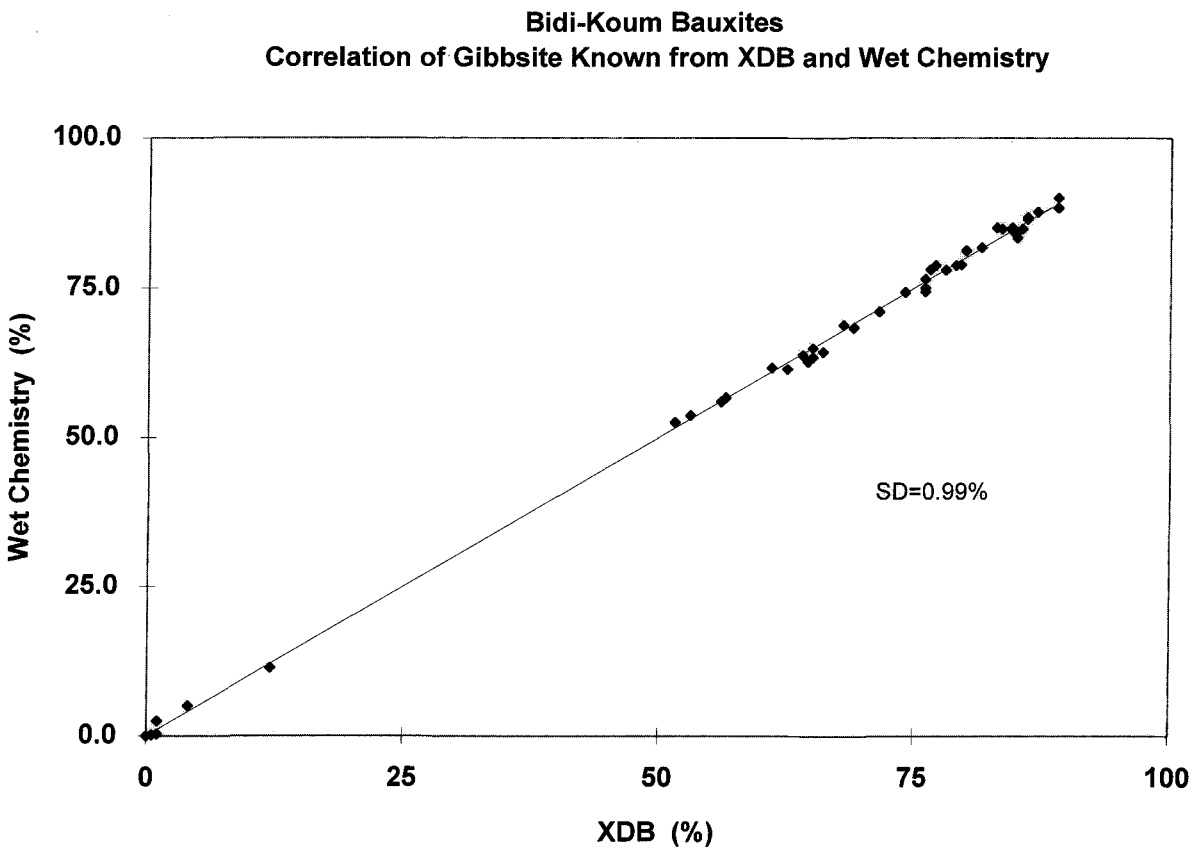


Figure 3. Bidi-Koum bauxites. Correlation of gibbsite known from XDB and wet chemistry.

Determination of Boehmite

In the laboratory high-temperature digestion, the sum of gibbsitic and boehmitic alumina, gb.Al_2O_3 (~225–235 °C), is used to describe alumina that passes into solution. This alumina is also known by the name "total extractable alumina" (TEA). Theoretically, this process dissolves not only gibbsitic and boehmitic alumina but also phosphate minerals, kaolinite, some quartz and probably some other minerals as well. Hence, the TEA determination is less accurate than, for example, the chemical g.Al_2O_3 determination, because it is based on several determinations each with its own analytical error. As a result, the so-called MONO (= boehmite) content that is calculated by the difference between TEA and g.Al_2O_3 is almost always higher than b.Al_2O_3 determined by a direct method, or obtained from the XDB method (Figure 4). Data compiled for Figure 4 confirmed that for the non-bauxitic samples BDK 34–38 and BDK 40, the present chemical methods provide erratic results. In a few cases, the XRD analysis did not justify any presence of boehmite, yet the chemical methods (applied outside of their appropriate range) reported meaningful concentrations.

The b.Al_2O_3 was determined for the samples BDK 34–52 directly following removal of gibbsite and kaolinite in a low-temperature caustic digestion. In order not to introduce any unnecessary bias in the calculations for samples BDK 1–33, the b.Al_2O_3 content corresponding to these samples was calculated using the equation:

$$\%\ b.Al_2O_3 = Al_2O_3 - g.Al_2O_3\ (\sim 150\ ^\circ C) - k.Al_2O_3(Ch) - i.Al_2O_3 - go.Al_2O_3 \quad [4]$$

where: Al_2O_3 = total Al_2O_3 (by XRF), k.Al_2O_3 = Al_2O_3 in kaolinite, i.Al_2O_3 = alumina in illite and go.Al_2O_3 = alumina in aluminum goethite (obtained from the XDB method).

Iron Minerals in Bauxites

It is important to know the quantity and nature of Fe minerals in bauxite, in order to predict the behavior of the ore during its processing. The Fe minerals are mainly hematite and goethite, and very seldom limonite and magnetite. There may also be some amorphous iron-bearing phases. Aluminum can replace Fe in the goethite structure, as has been shown by Norrish

https://doi.org/10.1346/CCMN.1997.0450311 Published online by Cambridge University Press

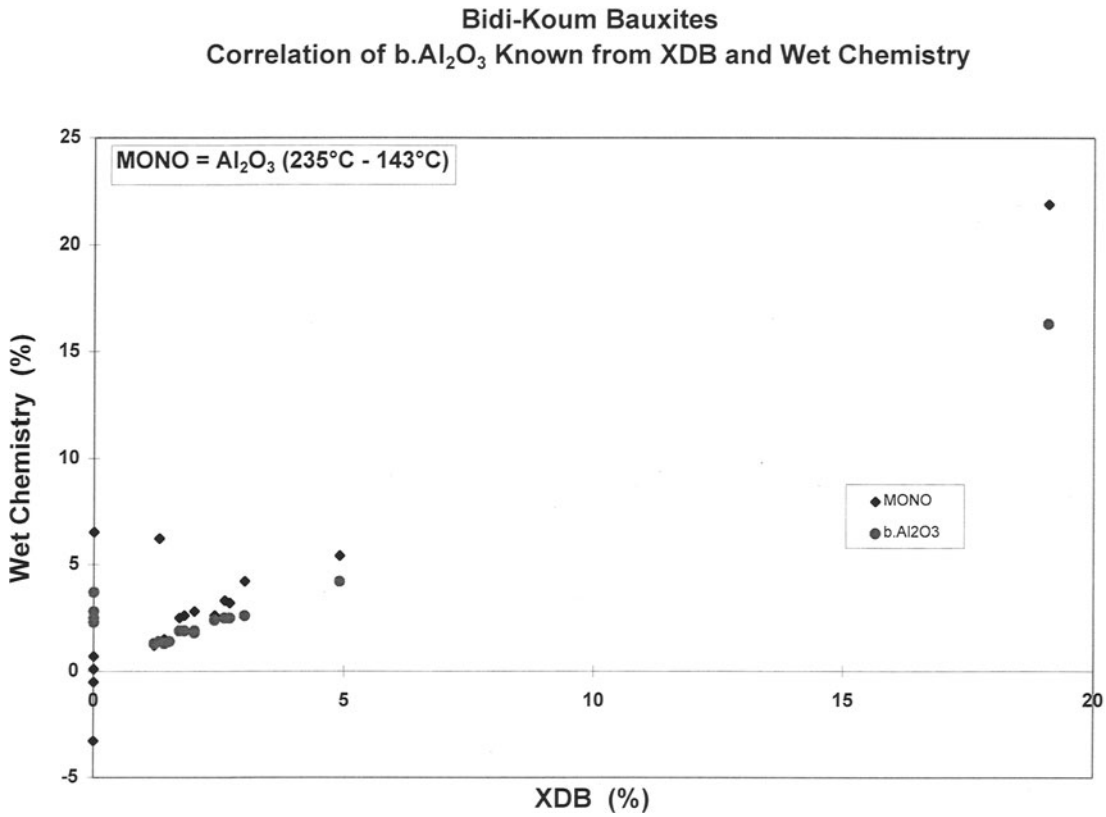


Figure 4. Bidi-Koum bauxites. Correlation of b.Al_2O_3 known from XDB and wet chemistry.

and Taylor (1961). The technological implication of this alumina is that it is not removed by caustic extraction under low-temperature Bayer plant digestion conditions (King 1971).

Thiel (1963) reported X-ray procedures for determining the mol% AlOOH isomorphorously substituting for FeOOH in the goethite lattice. He showed that the angular shift in the 2.44-Å (111) diffraction peak of goethite may be utilized to determine mol% AlOOH in the goethite structure. Another problem obstructing the XRD measurement of the iron oxides is variation of the mineral crystallinity. In general, goethite is finer than hematite. Goethite, as well as kaolinite, often gives rise to broad, ill-defined asymmetrical diffraction peaks so that there is always some uncertainty as to their position. The crystal size of hydrated Fe minerals in Jamaican bauxite, for example, does not exceed 50–60 Å (Verghese 1987). These particles, referred to as "colloidal iron", result in small and broad diffraction peaks not appropriate for quantitative mineral analysis. A portion of the Fe minerals less than 50 Å becomes "X-ray amorphous".

Bredell (1983) believes that the bulk of hydrated Fe oxides are present in bauxites in an amorphous hydrated state, yielding no XRD peaks. Therefore, the best approach in the calculation of goethite content seems to be when both XRF and XRD methods are employed. In Figure 5, distribution of hematite and goethite is presented for the Bidi-Koum samples. These data were obtained using the XDB software. In the Fe mass balance estimation, it was assumed that:

$$\%\ Fe_2O_3\ (\text{goethite}) = Fe_2O_3\ (\text{XRF}) - Fe_2O_3\ (\text{hematite}) \quad [5]$$

The hematite content was relatively well estimated using the diffractograms. Hematite crystals of very different morphology occur even for samples originating from the same deposit; this affects XRD measurement. Other possible sources of Fe contribution were simply ignored. It is highly unlikely that any significant Fe for Al substitution in boehmite (always at low concentration level) is possible. Two constituents of aluminum goethite, go.Al_2O_3 and go.H_2O, are presented in Figure 6 as a function of the 3rd constituent, go.Fe_2O_3. The amount of Al_2O_3 substitution in goethite was found from the goethite (110) peak maximum position.

It has to be noted that points representing hematite in Figure 5 and go.Al_2O_3 in Figure 6, which are out of linear relationships, correspond to the samples with

https://doi.org/10.1346/CCMN.1997.0450311 Published online by Cambridge University Press

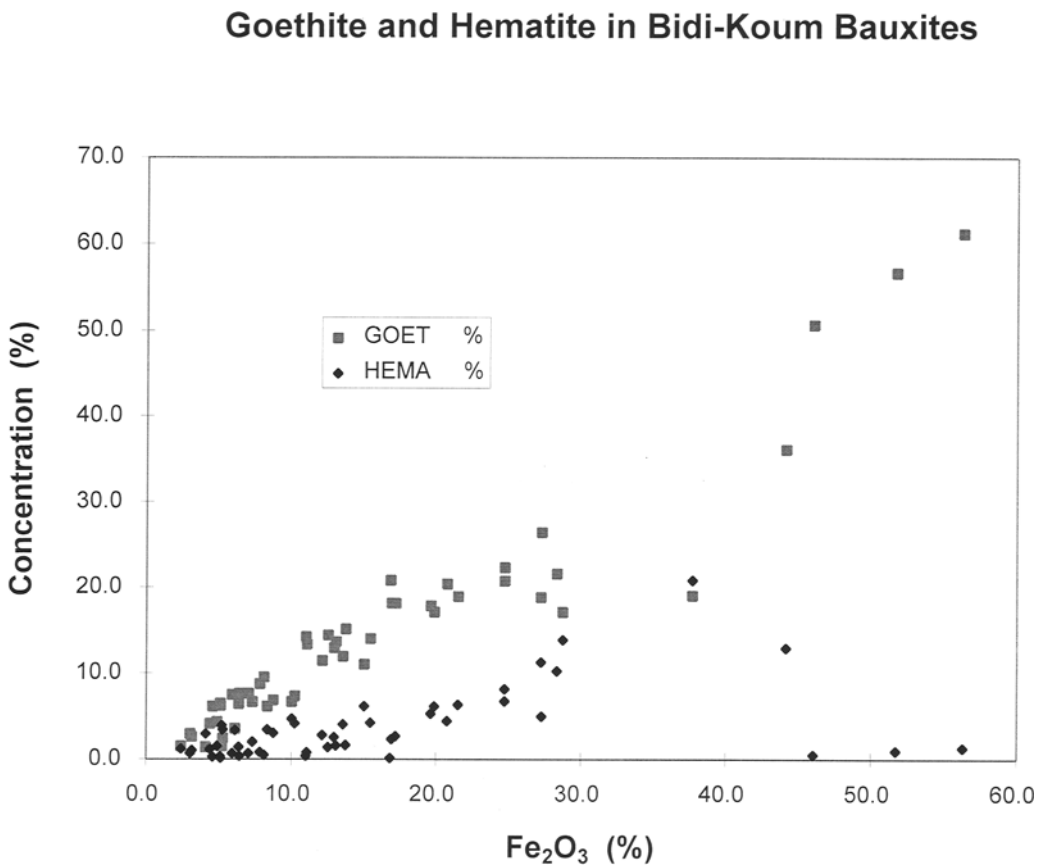


Figure 5. Goethite and hematite in Bidi-Koum bauxite.

low Al_2O_3. It means that, in the non-bauxitic samples, most or all of the Fe_2O_3 content is present as hematite. Simultaneously, the amount of Al_2O_3 substitution in goethite is very low or even none.

DISCUSSION

Data presented in this paper involve a large series of bauxite samples representing the same mineralogical deposit. It must be realized that the data obtained are based on the XRD quantification and the mass balance (assuming the stoichiometric composition of the considered mineral phases). Based on the comparison of wet chemical and XDB data, it is believed that the reported phase concentrations correspond well with reality.

From X-ray diffractograms we conclude that a majority of goethite and kaolinite in the Bidi-Koum bauxites occurs in an "X-ray amorphous" state which is not detected by XRD.

Much has been written about the displacement of *d*-values measured for goethite by XRD, but data to correlate the displacement and amount of Al_2O_3 substitution in the goethite lattice are scarce. The most reliable data for this correlation are those from Thiel (1963), obtained on a set of synthetic standards. Unfortunately, the *d*(110) line positions for these samples were not determined. As shown in this paper, it was possible to characterize Fe minerals in the Bidi-Koum bauxites using the XDB software.

It must be noted that other Fe compounds mentioned in the literature (Ni and Khalyapina 1978) and rarely found in bauxites, such as akaganeite (β-FeOOH) and lepidocrocite (γ-FeOOH), would contribute to the mass balance in the same way that goethite (α-FeOOH) does. There is a view that the ability of lepidocrocite to form solid solutions with Al_2O_3 is insignificant. Alternatively, maghemite (γ-Fe_2O_3) would make the same contribution to the mass balance as hematite (α-Fe_2O_3).

Among the secondary element oxides, ZrO_2 occurs at an average concentration of 0.1%, with the highest concentration of 0.23%. It is believed that ZrO_2 is associated with the mineral zircon ($ZrSiO_4$).

Phase concentrations determined using the XDB software alone were remarkably close to concentrations of selected phases obtained from wet chemical determinations (g.Al_2O_3, b.Al_2O_3, k.SiO_2). For example, in quantification of gibbsite, an average absolute

https://doi.org/10.1346/CCMN.1997.0450311 Published online by Cambridge University Press

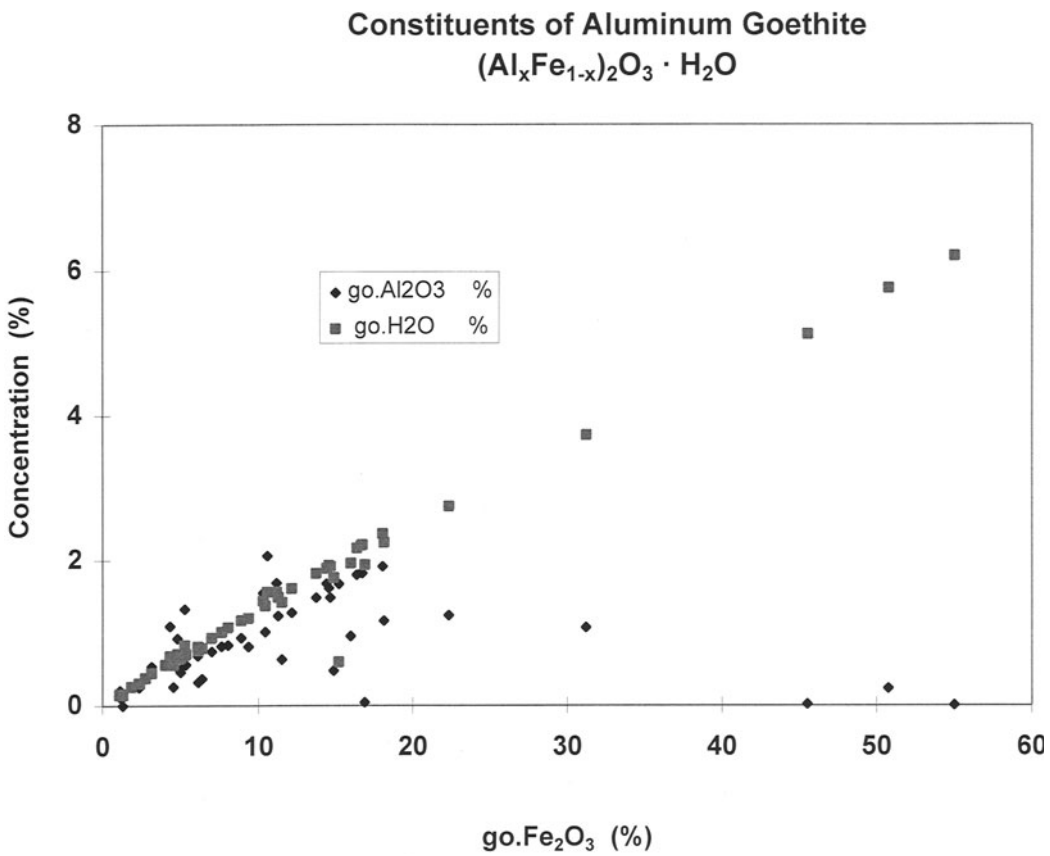


Figure 6. Constituents of aluminum goethite.

difference of about 1% was obtained between XDB and chemical concentrations over a broad concentration range. In addition to traditionally determined phases, such as gibbsite, boehmite and kaolinite, it was also possible to estimate the amounts of wavellite, goethite, hematite, quartz, rutile, anatase and illite in Bidi-Koum bauxites. Hence, the XDB software helps provide a much broader understanding of mineralogy of bauxites, and results in more accurate data interpretation. In addition, the XDB constitutes an interesting quality control and quality assurance tool for wet chemistry.

Using the XDB software, if the chemical concentration is known for at least 1 phase, the accuracy and reliability of determination of other phases improves.

REFERENCES

Andrews WH, Crisp AJ. 1980. Correlation of bauxite analysis with mineralogy. Light Met, AIME:3–18.

Bárdossy G. et al. 1980. Automated quantitative phase analysis of bauxites. Am Mineral 59:135–141.

Black HR. 1953. Analysis of bauxite exploration samples. Anal Chem 25:743–748.

Boski T, Herbillon AJ. 1988. Quantitative determination of hematite and goethite in lateritic bauxites by thermodifferential X-ray powder diffraction. Clays Clay Miner 36:176–180.

Bredell JH. 1983. Calculation of available alumina in bauxite during reconnaissance exploration. Econ Geol 78:319–325.

Feret F, Giasson GF. 1991. Quantitative phase analysis of Sangaredi bauxites (Guinea) based on their chemical composition. Light Met, AIME:187–191.

Feret F. 1993. Application of XRF in the aluminum industry. Adv X-ray Anal 36:121–137.

Hill RJ. 1992. Applications of Rietveld Analysis to materials characterization in solid-state chemistry, physics and mineralogy. Adv X-ray Anal 35:25–37.

King WR. 1971. The iron minerals in Jamaican bauxites. Light Met, AIME:3–18.

Montgomery O, deFoggi D. 1983. Rapid phase and chemical analysis. Light Met, AIME:15–20.

Ni LP, Khalyapina OB. 1978. Physical-chemical properties of the raw materials and products of alumina production. Alma-Ata, Kazakhstan: Izdatielstvo Nauka. 252 p.

Norrish K, Taylor RM. 1961. The isomorphous replacement of iron by aluminum in soil goethites. J Soil Sci 12:294.

Sajó I. 1994. Powder diffraction phase analytical system, Version 1.7, Users Guide. Budapest: Aluterv-FKI Ltd. 81 p.

Schorin H, Carias O. 1987. Analysis of natural and beneficiated ferruginous bauxites by both X-ray diffraction and X-ray fluorescence. Chem Geol 60:199–204.

Solymár K, Sajó I, Steiner J, Zöldi J. 1991. Characteristics and separability of red mud. Light Met, AIME:209–223.

https://doi.org/10.1346/CCMN.1997.0450311 Published online by Cambridge University Press

Strahl EO. 1982. Modern analytical methods in bauxite survey programs. In: Lyew-Ayee A, editor. Proc 5th Bauxite Symp. 188–203.

Taylor JC. 1991. Computer programs for standardless quantitative analysis of minerals using the full powder diffraction profile. Powder Diffr 6:2–9.

Thiel R. 1963. Goethite-diaspore system. Z Anorg u Allg Chem 326:70–78.

Verghese KI. 1987. The impact of impurities on the Bayer process. 8th Int Leichtmetalltagung; 1987; Leoben–Wien. p 42–46.

Young RA. 1993. The rietveld method. New York: Oxford Univ Pr. 298 p.

(*Received 28 December 1995; accepted 29 July 1996; Ms. 2725*)

https://doi.org/10.1346/CCMN.1997.0450311 Published online by Cambridge University Press